

## Photomechanical chemical microsensors

P.G. Datskos<sup>a,b,\*</sup>, M.J. Sepaniak<sup>b</sup>, C.A. Tipple<sup>b</sup>, N. Lavrik<sup>a</sup>

<sup>a</sup>Oak Ridge National Laboratory, 1 Bear Creek Road, P.O. Box 2008, Oak Ridge, TN 37831-8039, USA

<sup>b</sup>University of Tennessee, Knoxville, TN 37996, USA

### Abstract

Recently, there has been an increasing demand to perform real-time in situ chemical detection of hazardous materials, contraband chemicals, and explosive chemicals. The advent of inexpensive mass produced MEMS (microelectromechanical systems) devices has enabled the use of various microstructures for chemical detection. For example, microcantilevers were found to respond to chemical stimuli by undergoing changes in their bending and resonance frequency even when a small number of molecules adsorb on their surface. In our present studies, we extended this concept by studying changes in both the adsorption-induced stress and photo-induced stress as target chemicals adsorb or desorb on the surface of microcantilevers. We demonstrate that photo-induced bending of microcantilevers depends on the number of adsorbed molecules on their surface. On the other hand, microcantilevers that have undergone photo-induced bending will adsorb a different number of guest molecules. Depending on the photon wavelength and microcantilever material, the microcantilever can be made to bend by expanding or contracting a surface layer on one of its sides, unequally. Coating the surface of the microstructure with different materials can provide chemical specificity for the target chemicals. However, by choosing a handful of different photon wavelengths, tunable chemical selectivity can be achieved due to differentiated photo-induced response without the need for multiple chemical coatings. We will present and discuss our results on diisopropyl methyl phosphonate (DIMP), trinitrotoluene (TNT), two isomers of dimethylnaphthalene (DMN), tetrachloroethylene (TCE) and trichloroethylene (TRCE). © 2001 Elsevier Science B.V. All rights reserved.

**Keywords:** Microcantilevers; Microsensors; Trinitrotoluene (TNT)

### 1. Introduction

Present day chemical detection technologies are based primarily on adaptation of laboratory instruments. Over the past 20 years, a large number of spectroscopic methods that utilize optical absorption, light scattering, luminescence, atomic fluorescence or refractive index changes have been introduced. However, these methods rely on performing laboratory chemical analysis on extracted samples and provide no real-time data for operational feedback, are generally expensive and complicated to use.

Recently, there has been an increasing demand to perform real-time in situ chemical detection of hazardous materials, contraband chemicals, and explosive chemicals. Simple, effective and easy to use chemical sensors are desirable for these purposes. Gravimetric chemical sensors achieve chemical specificity due to chemically selective coatings [1,2]. Such coatings have been used in different types of gravimetric sensors to sorb various gaseous analytes. The

advent of inexpensive mass produced MEMS (microelectromechanical systems) devices has enabled the use of various microstructures for chemical detection. Microcantilever-based chemical sensors were found to respond to chemical stimuli by undergoing changes in their bending and resonance frequency even when a small number of molecules adsorb on their surface [3–9]. The response of a microcantilever to chemical stimuli is depicted schematically in Fig. 1. Surface stresses  $s_1$  and  $s_2$  are balanced at equilibrium, generating a radial force along the medial plane of the microcantilever. When molecules adsorb on a microcantilever surface they affect  $s_1$  and  $s_2$  unequally. Change in a differential stress  $s_2 - s_1$  produces an additional bending force that displaces the tip of the microcantilever to a new position. Previous work has shown that microcantilever bending can readily be determined by a number of means, including optical, capacitive, piezoresistive, and electron tunneling with extremely high sensitivity [10]. For example, the metal-coated microcantilevers that are commonly employed in atomic force microscopy (AFM) allow sub-Angstrom ( $<10^{-10}$  m) sensitivity to be routinely obtained. Hansma [11] and Binnig [12] have demonstrated AFM sensitivities of  $10^{-11}$  N, corresponding to bending magnitudes

\* Corresponding author. Tel.: +1-865-574-6205; fax: +1-865-574-9704.  
E-mail address: pgd@ornl.gov (P.G. Datskos).

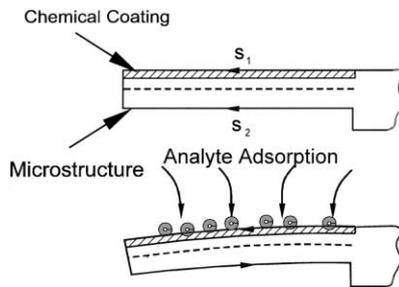


Fig. 1. Schematic diagram depicting the bending response of a microcantilever to chemical adsorption. Surface stresses,  $s_1$  and  $s_2$  are balanced at equilibrium, but become unequal and cause bending upon adsorption of analyte molecules. A force along the  $z$ -direction is induced due to the differential surface stress, which causes the microcantilever to change its radius of curvature.

of approximately  $5 \times 10^{-11}$  m. More recently, even smaller microcantilever deflections were measured with a resolution of  $0.4 \times 10^{-12}$  m [13]. Standard AFM microcantilevers are typically 100–200  $\mu\text{m}$  long, 0.3–3  $\mu\text{m}$  thick and 10–30  $\mu\text{m}$  wide, and can be fabricated from various dielectric or semiconducting materials. Microcantilevers made out of GaAs were also fabricated with a thickness of merely 100 nm [14]. When even thinner microcantilevers were used, measurements of  $10^{-18}$  N have been reported. Microcantilevers can be mass produced at relatively low cost using standard semiconductor manufacturing methods.

In this work, we extended the simple microcantilever-based chemical detection by studying changes in both the adsorption-induced stress and photo-induced stress as target chemicals adsorb or desorb on the surface of microcantilevers. By combining photo- and chemically-induced bending we introduced a novel method to detect and monitor stress changes in bimaterial microcantilevers due to the adsorption of molecules. Indeed, microcantilevers that have adsorbed molecules will undergo photo-induced bending that depends on the number of adsorbed molecules on the surface; on the other hand, microcantilevers that have undergone photo-induced bending will adsorb guest molecules differently. This is important in cases, where the photo-induced stresses can be used to counter adsorption-induced stresses and, thus, increase the dynamic range. Depending on the photon wavelength and microcantilever material, the microcantilever can be made to bend by expanding or contracting a surface layer on one of its sides. Coating the surface of the microstructure with a different material can provide chemical specificity for the target chemicals. However, by choosing a handful of different laser diode wavelengths an increase in the chemical selectivity can be achieved due to differentiated photo-induced response without the need for different surface coatings. One can also obtain a photothermal spectrum by exposing microcantilevers to photons with different wavelengths. In this case, the chemical detection is based on the ability to detect small changes in the temperature of the

microcantilevers due to interaction of the adsorbate with the probing photons.

In the present studies, we explored photo-induced and absorption induced stresses in microcantilevers coated with gold layers, self-assembled monolayers, and organic coatings that exhibit molecular recognition properties.

## 2. Molecular adsorption on microcantilevers

### 2.1. Chemical detection based on micromechanical photon-induced stress

Using bimaterial micromechanical structures that undergo bending due to interaction with both photons and molecular species, we have developed a new chemical sensing technique. It is known that microcantilevers undergo bending following the absorption of photons [15–18]. In fact, direct “quantum mechanical” conversion of optical power to mechanical motion offers a number of advantages over other indirect optical or non-optical approaches [19]. Our particular approach is based on the fact that this photo-induced bending of microcantilevers depends on the amount of chemical analyte adsorbed on a microcantilever surface. For the same number of photons interacting with the microcantilever, its photo-induced bending will vary if the amount of molecular species adsorbed on its surfaces changes. Earlier work has shown that the absorption of photons by a solid results in temperature changes and thermal expansion which, in turn, gives rise to acoustic waves at frequencies corresponding to the amplitude modulation of the probing photon beam [16,17]. It is well known that generation of “free” charge carriers (electrons and holes) via absorption of photons in a semiconductor results in a local mechanical strain [15–18,20]. It should be emphasized that this photo-induced strain is additional to the strain resulting from unequal thermal expansion of the semiconductor and metal. In fact, for the same power of photo-irradiation, a gold-coated silicon microcantilever exhibits a photo-induced bending that is about 4 times larger than that due to thermally induced stress. For a rectangular semiconductor bar (Fig. 2) of thickness,  $t$ , length,  $l$  and energy bandgap,  $\epsilon_g$ , the change in bending due to changes in the density of photogenerated charge carriers,  $\Delta n$ , and changes in temperature,  $\Delta T$ , will be the sum of the photo-induced component and the thermal component viz. [21]

$$z_{\max} \approx \frac{(1-\nu)l^2}{t} \frac{d\epsilon_g}{dP} \Delta n + \frac{3(1-\nu)l^2}{t} \alpha \Delta T \quad (1)$$

where  $\nu$  is Poisson’s ratio,  $d\epsilon_g/dP$  the pressure dependence of the energy bandgap,  $\alpha$  the coefficient of thermal expansion, and  $E$  the Young’s modulus. The first term inside of Eq. (1) is due to photo-induced surface stress and the second term is due to thermal stress caused by temperature changes. Assuming that a radiant power,  $\Phi_e$  absorbed by a semiconductor microcantilever with mass,  $m$  and heat capacity,  $c_p$

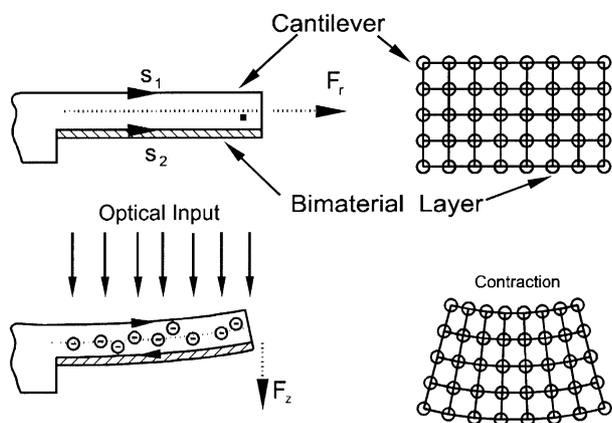


Fig. 2. Schematic diagram showing the bending process of a semiconductor microcantilever exposed to photons. Surface stresses,  $s_1$  and  $s_2$  are balanced at equilibrium. Also depicted is the accompanied expansion of the semiconductor lattice following the generation of electron pairs.

generates number density of excess charge carriers,  $\Delta n$ , we get [18]

$$z_{\max} \approx \frac{(1-\nu)l^2}{t} \left( \eta \frac{\lambda d\epsilon_g}{hc dP} \frac{1}{lwt} + \frac{3\alpha}{mc_p} \right) \tau_L \Phi_e \quad (2)$$

where  $\eta$  is the quantum efficiency,  $h$  ( $= 6.625 \times 10^{-34}$  J s) is Planck's constant,  $c$  ( $= 3 \times 10^8$  m s $^{-1}$ ) the speed of light,  $m$  and  $c_p$ , the microcantilever mass and the heat capacity, respectively, and  $\tau_L$  the lifetime of the carriers in the semiconductor.

When the photo-induced bending is used as the detection method, the chemical coating does not have to be restricted to only one surface as in commonly used microcantilever-based chemical sensors [4,5,7–9,22–26]. Coating both sides with a chemically sensitive layer will essentially increase (double) the effective area available for adsorption of analytes. Since these microstructures are also very sensitive temperature sensors, care should be taken to account for bending due to heat dissipation. One approach would be to employ reference microcantilevers that are not exposed to analytes and perform differential measurements. The actual photo-induced bending of microcantilevers exposed to chemical analytes can be measured with a number of techniques originally developed for scanning force microscopy (see later Section 3).

### 2.2. Chemical sensing based on microcantilever resonance frequency

Currently available gravimetric chemical sensors [1,27] such as quartz crystal microbalances [28], surface acoustic wave (SAW) [29], acoustic plate mode (APM) devices [30], chemiresistors [1], and flexural plate wave oscillators (FPW) [31] achieve sensing by monitoring the sorption processes on the sensing element that result in some frequency shift. When the interaction of an analyte with the microcantilever

results in the adsorption of that species on the microcantilever surface, it causes changes in the deflection (or radius of curvature) and the resonant frequency,  $f_0$ , of the microcantilever. For a rectangular microcantilever bar with a spring constant,  $k$ , the resonance frequency,  $f_0$ , is inversely proportional to the square root of the effective mass,  $\Delta m_{\text{eff}}$  of the microcantilever ( $f_0 = (1/2\pi)(k/m_{\text{eff}})^{1/2}$ ). The effective mass can be related to the mass of the microcantilever,  $m$ , through the relation:  $m_{\text{eff}} = nm$ , where  $n$  is a geometrical factor [6,10]. For example, in the case of commercially available silicon nitride microcantilevers with spring constants of 0.06 and 0.03 N/m, the values of  $n$  are 0.14 and 0.18, respectively [6]. In order to determine the change in resonance frequency,  $\Delta f(m_{\text{eff}}, k)$ , both the change in spring constant,  $\Delta k$ , and the change in mass,  $\Delta m_{\text{eff}}$  should be taken into account. For instance, a change of  $\Delta k/k$  of  $10^{-6}$  was reported for gelatin coated microcantilevers [4].

### 2.3. Chemical sensing using microcantilever bending changes

The bending of a microcantilever is extremely sensitive to the adsorption of chemical analytes on its surface. Our results show that monitoring of the bending as analytes adsorb on the microcantilever surface can provide the highest chemical sensitivity. The detectable mass can be two orders of magnitude smaller when, instead of the resonance frequency change, the microcantilever bending is used as the chemical sensing mechanism. As microcantilevers are stressed (for example, due to adsorption of a chemical analyte) a change in its radius of curvature,  $R$  (see Fig. 1) occurs. The corresponding bending,  $z_{\max}$  ( $=l^2/(2R)$ ) of the microcantilever can be expressed as [32–34]

$$z_{\max} = \frac{3l^2(1-\nu)}{Et^2} \Delta s \quad (3)$$

where  $\nu$  is the Poisson's ratio and  $\Delta s = s_2 - s_1$ , the differential surface stress.

If one side of the microcantilever is relatively passive (i.e. non-adsorbing), the changes in  $\Delta s$  are caused primarily by the modulation of Gibbs surface free energy of the adsorbing side. The surface free energy can be evaluated using a modification of the Young–Dupré relationship for the substrate-coating system given by

$$S_2 = \sigma_{\text{sub}} + \sigma_{\text{coat}} - W_{\text{adh}} - W_{\text{ster}} \quad (4)$$

where  $\sigma_{\text{sub}}$  and  $\sigma_{\text{coat}}$  are the surface tensions of the free substrate and the chemical coating, respectively,  $W_{\text{adh}}$  the work of adhesion between the coating and the substrate, and  $W_{\text{ster}}$  accounts for the energy of possible steric repulsive forces between molecules in the coating. Note that  $W_{\text{adh}}$  is a normalized value that accounts for the surface density of modifying molecules. For occupancies up to a closely packed monolayer,  $W_{\text{adh}}$  is nearly proportional to the binding energy per receptor molecule and the density of the receptor

on the microcantilever surface.  $W_{\text{adh}}$  can be further described as

$$W_{\text{adh}} = E_{\text{adh}} \frac{m_s}{M} \quad (5)$$

where  $E_{\text{adh}}$  is the binding energy per mole,  $m_s$  the surface mass and  $M$  the molar mass of the modifying material. In the case of a noble metal substrate and an organic modifying coating,  $\sigma_{\text{sub}} \gg \sigma_{\text{coat}}$ . In this case, the change in bending is given by

$$z_{\text{max}} = \frac{3l^2(1-\nu)}{Et^2} \left( \sigma_{\text{sub}} - s_1 - E_{\text{adh}} \frac{m}{M} - W_{\text{ster}} \right) \quad (6)$$

We should point out that when receptor molecules are very densely packed on the microcantilever surface, or in the case of thicker (multilayer) modifying coatings and/or nanostructured surfaces, analyte binding can induce differential surface stress through additional mechanisms not discussed here.

#### 2.4. Microcalorimetric spectroscopy detection

Photomechanical chemical detection can also be enhanced using microcalorimetric spectroscopy technique [35]. This spectroscopic technique relies on measurement of minute changes of the microcantilever as a function of probing wavelength. The mechanisms of such changes include absorption of energy of the probing beam by analyte molecules on microcantilever surfaces. Therefore, photothermal spectra are similar to conventional infrared spectra and can be used to provide information on the chemical composition of the analyte. A unique photothermal spectrum can be obtained for submonolayer coverages of the analyte on the microcantilever. Chemical detection based on microcalorimetric spectroscopy is capable of detecting and identifying chemical analytes present at both very low and very high concentrations. We have applied this technique to the detection of diisopropyl methyl phosphonate (DIMP), trinitrotoluene, and toluene.

Below, we briefly describe the basic steps of microcalorimetric spectroscopy. Fig. 3 shows the concept of microcalorimetric spectroscopy schematically. The detection of the presence and identification of molecules using microcalorimetric spectroscopy can be broken down into two main steps. In the first step, the sample is allowed to interact with the surface of a micromechanical thermal detector (with femtojoule sensitivity) that is coated with an appropriate chemical layer selective to the family of the target chemicals. By scanning a broadband wavelength region with the aid of a monochromator, a photothermal spectrum of the molecules adsorbed on the detector surface is obtained in the second step. The magnitude of wavelength-dependent temperature changes is proportional to the number of molecules adsorbed on the detector surface. Although, highly selective chemical coatings are generally desirable, microcalorimetric spectroscopy can provide an

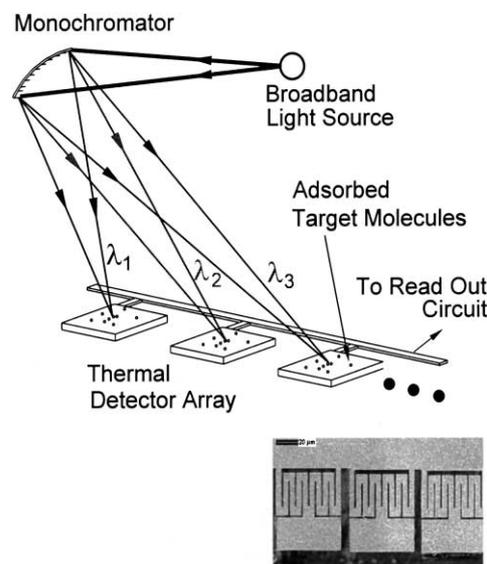


Fig. 3. Schematic representation of the principle of microcalorimetric spectroscopy technique. Photons of different wavelength irradiate different thermal detectors configured as a linear array. Molecules adsorbed on the surface of thermal detector elements absorb photons and a photothermal spectrum is obtained.

attractive means to achieve chemical detection with less selective chemical layers.

### 3. Experimental

Although bending of microcantilevers can readily be determined by a number of means (optical [10], capacitive [36], electron tunneling [10], and piezoresistive methods [10,37]) in this work, we focused on optical readout techniques. The approach used was adapted from standard atomic force microscopy imaging systems. The experimental setup is shown in Fig. 4 and is described in detail,

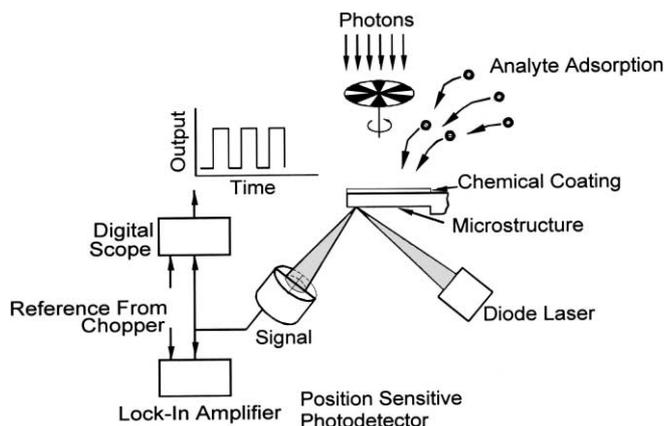


Fig. 4. Schematic of the setup that will be used to determine the photo-induced bending of microcantilevers exposed to analytes. In this arrangement, the diode laser with  $\lambda = 790$  nm (or 1400 nm) is used to produce the photo-induced bending and the diode laser with  $\lambda = 633$  nm is used to measure the deflection of the microcantilever.

elsewhere [8,24]. Microcantilevers were placed into a measurement cell and  $N_2$  gas was used as the carrier gas. Analyte molecules diluted in nitrogen were delivered into the cell through a 4-way valve, which enabled switching between analyte/ $N_2$  mixture and the pure carrier gas. A syringe pump was used to inject saturated analyte vapors into a flow system at a controllable rate. A ratio of the analyte injection rate to a total flow rate defined a degree of analyte dilution. The total flow rate was measured at the cell outlet using a mass flowmeter tube. Modification of the microcantilevers with three distinctive types of chemically selective coatings are described below.

We formed the self-assembled composite monolayer based on thiol–gold chemistry as procedure described elsewhere [38]. After a surface cleaning procedure, the microcantilevers were placed in the 1 mM 11-mercaptoundecanoic acid/hydrogen peroxide solution for 8–12 h. The chemical process ceases when a highly ordered monomolecular layer of carboxylate-terminated alkanethiol is formed on a gold-coated side of the microcantilever. Then, the microcantilevers were rinsed with ethanol and water and were placed in a 2 mM solution of copper (II) perchlorate hexahydrate in ethanol for about 5–10 min, which results in binding of copper (II) ions to the surface of the thiol monolayer. The copper (II) ions allowed for selective and reversible binding of organophosphonate molecules such as DIMP.

In order to chemically modify a gold-coated side of the microcantilevers, we also used thiol-derivatized  $\beta$ -cyclodextrin. This synthetic receptor is known to exhibit molecular recognition properties with respect to certain organic analytes and can be conveniently used to create covalently-attached monoayers on gold. For our experiments, gold-coated silicon nitride microcantilevers were immersed in a 1 mM solution of per-6-thio- $\beta$ -cyclodextrin in DMSO/ $H_2O$  (3:2) for 18 h. The microcantilevers were subsequently rinsed with the mixture DMSO/ $H_2O$  mixture.

The third type of chemically selective coatings that we have tested in this study is thermally evaporated films of calixarene derivatives. Calix[ $n$ ]arenes are macrocyclic cavitands which are able to interact selectively with both charged and neutral guest molecules. Many of calix[ $n$ ]arene derivatives can readily be deposited on solid substrates using thermal evaporation in vacuum. We have selected calix[4]arene because of its high affinity to smaller molecules of chlorinated nonaromatic organic solvents. In particular, high sensitivity of calix[4]arene coatings to chlorinated ethylene derivatives can be expected [39,40]. 4-*tert*-Butylcalix[4]arenes (Acros Organics) was evaporated onto  $SiN_x$  microcantilevers using a Cooke 200 evaporator equipped with a resistance heater, a quartz crucible and a QCM thickness monitor. The deposition rate of 0.02–0.05 nm/s was maintained during the deposition procedure.

In the photomechanical studies we used microcantilevers as photon detectors [41,42]. The microcantilever photon detectors were exposed to photons from a laser source or

to IR radiation from the spectrometer prior to any exposure to chemicals and their thermal response was recorded as a function of photon wavelength. The wavelength region (2.5–14.5  $\mu\text{m}$ ) attainable with our spectrometer (Foxboro Miran-80 IR spectrometer) was divided into three regions: (i) 2.5–4.5  $\mu\text{m}$ ; (ii) 4.5–8.0  $\mu\text{m}$ ; and (iii) 8.0–14.5  $\mu\text{m}$ . The thermal detectors were exposed to chemical analytes and a new thermal response was recorded as a function of photon wavelength. The increase in thermal response of the detector at particular wavelengths was attributed to the absorption of photons by the molecules adsorbed on the thermal detector surface. All measurements were conducted at ambient temperature and atmospheric pressure.

## 4. Results and discussion

### 4.1. Adsorption-induced studies

#### 4.1.1. Modified *n*-alkanethiol self-assembled monolayers (SAMs)

We used gold-coated Si microcantilevers to investigate the effect of adsorbed diisopropyl methylphosphonate (DIMP) on photo-induced bending of microcantilevers. DIMP is a phosphorous containing organic chemical which is used as a model for chemical warfare agents. Microcantilevers with  $Cu^{2+}$  terminated SAM coatings were exposed to DIMP by injecting DIMP vapor into a cell with the microcantilever sensor. The composite monolayer coating on the microcantilever adsorbs DIMP molecules reversibly causing the microcantilever to deflect in proportion to the analyte concentration (see Fig. 5). The response time is rather fast and depends on the flow rate of the  $N_2$  carrier gas. A flow rate of 50 ml/min was used to obtain the data shown in Fig. 5.

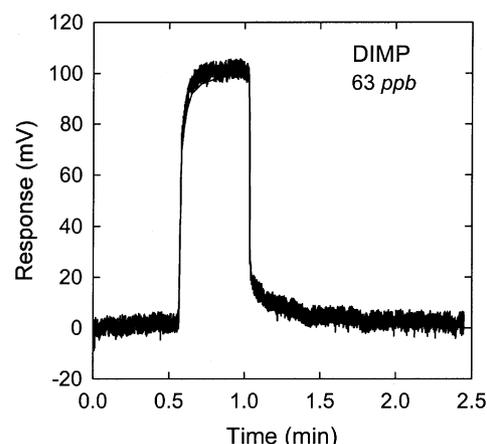


Fig. 5. Bending response of microcantilevers with  $Cu^{2+}$  bound on a carboxylate-terminated *n*-alkanethiol monolayers exposed to DIMP. During the exposure time, no measurable change in the resonance frequency was observed.

The selectivity of the observed responses relies on the high affinity of organophosphonate compounds to terminal  $\text{Cu}^{2+}$  groups bound to the SAM. Previously Kepley et al. [38] used the same type of  $\text{Cu}^{2+}$ -terminated chemical coating on a QCM device and based their choice on the fact that  $\text{Cu}^{2+}$  and some of its chelates are hydrolysis catalysts for certain chemical warfare agents. Although, unmodified gold surfaces may also interact with DIMP, the efficiency and selectivity of such interactions are poor [38]. Our observations using microcantilever transducers confirm that a chemical surface layer of coordinatively unsaturated  $\text{Cu}^{2+}$  can provide both selective and reversible binding sites for organophosphonate compounds.

#### 4.1.2. $\beta$ -Cyclodextrin SAMs

$\beta$ -Cyclodextrin modified microcantilevers were placed in the flow cell and exposed to analyte vapors diluted in a stream of the carrier gas ( $\text{N}_2$ ). Fig. 6 shows typical responses of the  $\beta$ -cyclodextrin modified microcantilever to vapors of a series of organic compounds. Exposure of the functionalized microcantilever to the analyte for 2 min was followed by purging the cell with pure carrier gas for 5–10 min. Diluted vapor of each of the selected analytes was used in order to obtain the responses shown in Fig. 6. Diluted vapors of 1,8-dimethylnaphthalene (1,8-DMN) and 2,7-dimethylnaphthalene (2,7-DMN) caused responses shown in Fig. 6 by curves (a) and (b), respectively. The next two responses (curves (c) and (d) in Fig. 6) were caused by diluted vapors of tetrachloroethylene (TCE) and trichloroethylene (TRCE). The differences in magnitudes of the responses reflects the coated microcantilever selectivity. The higher magnitude of the response to 1,8-DMN as compared to 2,7-DMN correlates well with the model of inclusion complexes of  $\beta$ -cyclodextrin and different DMN isomers. The 1,8-DMN molecule is less elongated than 2,7-DMN and, thus, causes the cyclodextrin to distort more upon the complexation. The sensitivities of 1,8-DMN and 2,7-DMN were determined to be 11.2 and 22.0 nm deflection per ppb,

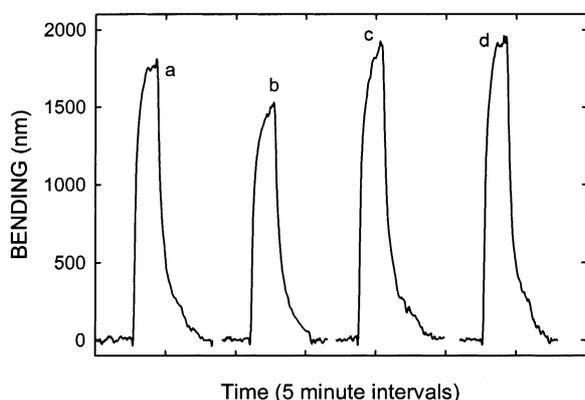


Fig. 6. Bending response of  $\beta$ -cyclodextrin modified microcantilevers to (a) 196.6 ppb of 1,8-dimethylnaphthalene; (b) 83.0 ppb 2,7-dimethylnaphthalene; (c) 201.8 ppm tetrachloroethylene; and (d) 680.2 ppm trichloroethylene.

respectively. Comparison of the responses to TCE and TRCE (curves (c) and (d) in Fig. 6) reveals lower sensitivity of the  $\beta$ -cyclodextrin modified microcantilevers to these chlorinated compounds. The lower sensitivity can be explained by the fact that the molecules of TCE and TRCE are smaller than the  $\beta$ -cyclodextrin cavity and their complexation is less favorable than in the case of the DMNs. The deflection sensitivities of  $\beta$ -cyclodextrin modified microcantilevers to TCE and TRCE were determined to be 11.5 and 3.4 nm per ppm, respectively. We estimated respective limits of detection (LOD) using linear regressions of the calibration plots obtained for each analyte. A concentration at which the extrapolated response exceeds the noise level 3 times was accepted as a value of LOD. A typical noise level of the monitored microcantilever deflections was 20 nm. The calculated LODs for 1,8-DMN, 2,7-DMN, TCE and TRCE were determined to be 5.3 ppb, 2.7 ppb, 5.2 ppm, and 17.5 ppm, respectively.

#### 4.1.3. Evaporated calixarene coatings

Microcantilevers with 75 nm calixarene coatings were investigated for their response to TCE. The responses of the microcantilevers to TCE were measured in 1 ml flow cell. Fig. 7 shows typical responses obtained with calix[4]-arene coated Si microcantilevers in presence of TCE. Each response in Fig. 7, was induced by switching the cell to a flow of TCE/ $\text{N}_2$  mixture for 10 min. Purging the cell with pure nitrogen correspond to the recovery regions. A constant gas flow of  $3 \pm 0.5 \text{ ml min}^{-1}$  was maintained during the whole experiment. Using a linear regression of the obtained calibration plots (Fig. 8) and the value of measured noise level (20 nm) the LOD for TCE was found to be 1.13 ppm.

#### 4.2. Photomechanical studies

In our studies we also used gold-coated microcantilevers to investigate photomechanical chemical sensing and the effect of molecular adsorption on the photo-induced bending

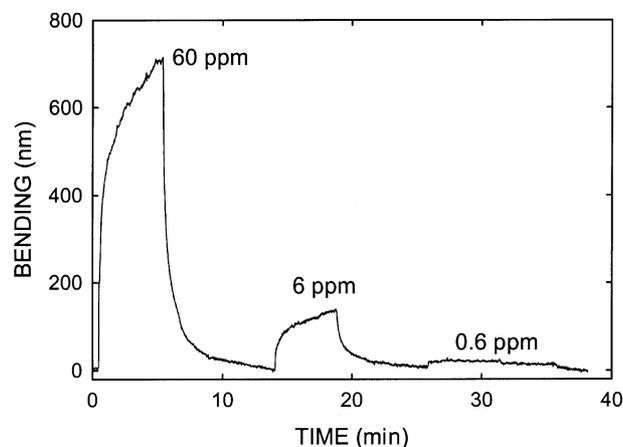


Fig. 7. Bending response of calix[4]arene coated silicon microcantilevers to TCE.

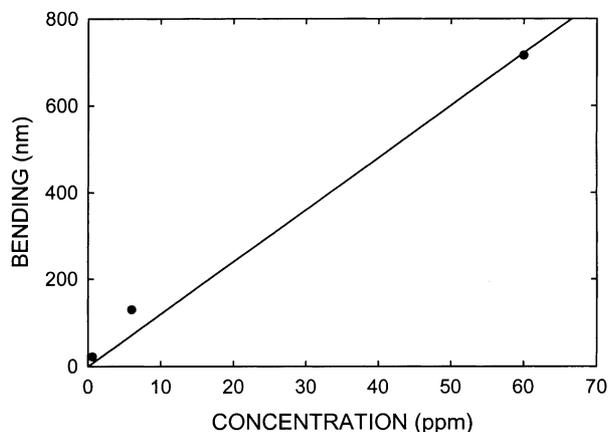


Fig. 8. Bending response of calix[4]arene coated silicon microcantilevers as a function of concentration of trichloroethylene.

of microcantilevers. Depending on the photon wavelength and microcantilever material, the bending can be in either direction.

We used diisopropyl methylphosphonate (DIMP) which has a vapor pressure of  $\sim 700$  mTorr at  $25^\circ\text{C}$ . DIMP is a phosphorous containing organic chemical which is used as a model for chemical warfare agents. A number of gravimetric-based transducers have been used previously as platforms for detecting analogous phosphorous organic compounds. An earlier study [38] has used a SAW device with SAMs to achieve selectivity and reversibility. In the present studies, we exposed DIMP directly to gold-coated microcantilevers both for simplicity and because gold reflects most of the incoming IR energy minimizing direct heating of the substrate.

We measured the photo-induced bending of a gold-coated Si microcantilever exposed (Si side) to a 790 nm diode laser

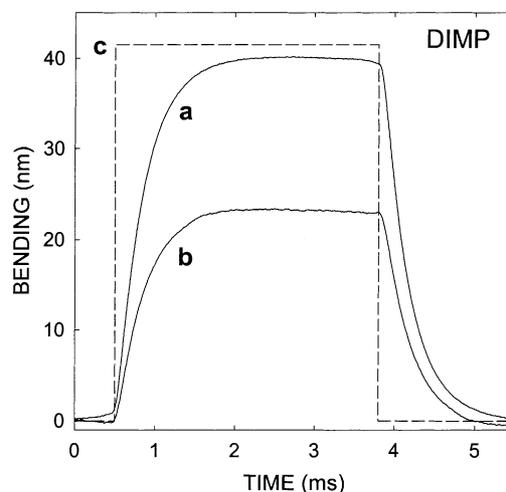


Fig. 9. Photo-induced bending of (a) a gold-coated microcantilever with no analytes adsorbed; and (b) same microcantilever as before, but exposed to DIMP. The dashed curve (c) shows the amount of time the microcantilever was exposed to photons that caused the photo-induced bending observed. During the exposure time, no measurable change in the resonance frequency was observed.

and obtained the photomechanical response shown in Fig. 9 by curve (a). We subsequently exposed the gold-coated microcantilever to DIMP. Following the adsorption of DIMP molecules, the microcantilever was exposed to photons using a diode laser (790 nm, and same intensity as before) and again measured the photo-induced bending shown by curve (b) in Fig. 9. During the exposure of the microcantilever to DIMP we did not detect any changes in the resonance frequency ( $<0.1$  Hz) of the microcantilever which puts a limit on the adsorbed mass of less than  $1 \times 10^{-9}$  g/cm<sup>2</sup>.

In Fig. 10, we plotted the photothermal response of a microcantilever thermal detector from 8.0 to 14.5  $\mu\text{m}$  with

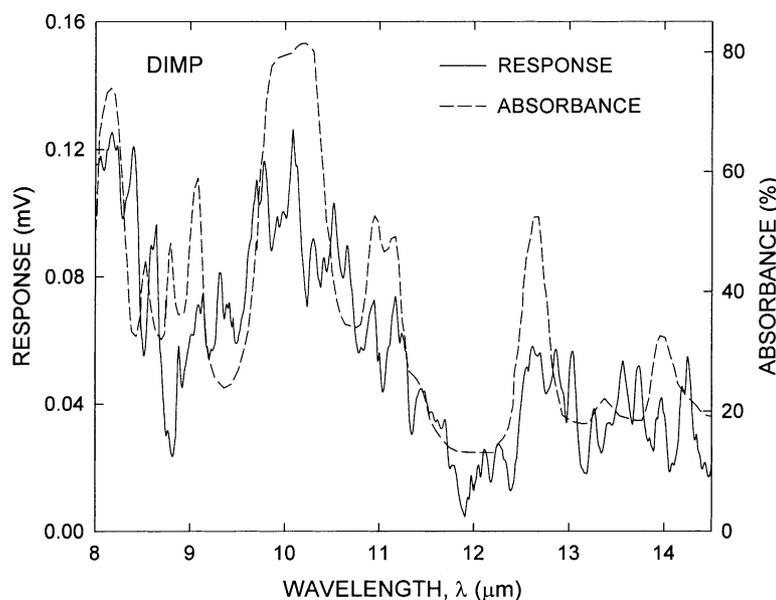


Fig. 10. DIMP photothermal spectrum from 8.0 to 14.5  $\mu\text{m}$  obtained using a gold-coated microcantilever detector with molecules adsorbed on its surface (solid curve). Also plotted is the IR spectrum of DIMP (dashed curve).

DIMP molecules adsorbed on its surface (solid curve). The microcalorimetric (photothermal) spectrum was obtained with about one monolayer of coverage. Also plotted in Fig. 10 is the infrared absorption spectrum of DIMP between 8.0 and 14.5  $\mu\text{m}$  (dashed curve). The peaks in the photothermal spectrum of DIMP shown in Fig. 10 correspond well with the absorption peaks in the IR spectrum of DIMP (Fig. 10, dashed curve). Since, DIMP molecules absorb photons at these wavelengths, their internal energy increases as molecules populated higher vibrational levels. The internal energy of each DIMP molecule is dissipated either by radiation, convection or conduction to the gold substrate. It is the heat of conduction from the “hot” molecules to the gold substrate of the microcantilever that increases the temperature of the microcantilever causing it to bend. Our present results demonstrate that it is possible to detect less than a submonolayer of DIMP coverage using microcalorimetric spectroscopy.

Since DIMP molecules absorb photons at these wavelengths, their internal energy increases as molecules populated higher vibrational levels. The internal energy of each DIMP molecule is dissipated either by radiation, convection or conduction to the gold substrate. It is the heat of conduction from the “hot” molecules to the gold substrate of the microcantilever that increases the temperature of the microcantilever causing it to bend.

TNT was a second analyte selected for our studies. TNT is solid at room temperature, has very low vapor pressure ( $10^{-6}$  Torr) and its detection under ambient conditions presents a challenge. In our studies, we exposed gold-coated Si microcantilevers to TNT molecules in order to investigate the effect of photo-induced stress. Because of the very low vapor pressure a minute quantity of TNT molecules could be adsorbed on the surface. Consequently, a very small adsorption-induced stress was expected. In fact, we found no measurable response to TNT due to any adsorption-induced stresses alone. Using a 10 mW HeNe laser, we measured the photo-induced stress both before and after exposure to TNT. The exposure of the gold-coated microcantilever to TNT was provided by placing less than 5 mg of TNT into the chamber housing the microcantilever. Afterwards, TNT sample was removed from the chamber and the measurements of photo-induced stresses were carried out again. Fig. 11 shows the photo-induced response of the microcantilever prior to exposure to TNT (curve a) and after exposure to TNT (curve b). Fig. 11 shows that the photo-induced bending depends on the presence of TNT molecules on the surface. Since Si contracts when exposed to 633 nm photons, the photo-induced bending decreases as more TNT molecules adsorb on the surface of our detector. We attribute our findings to changes in the surface states of the gold-coated microcantilever due to adsorption of TNT molecules.

We also studied thermal responses of microcantilever thermal detectors with TNT molecules adsorbed on their surface. In analogy to the previous experiments, TNT was placed in a chamber containing a platinum-coated

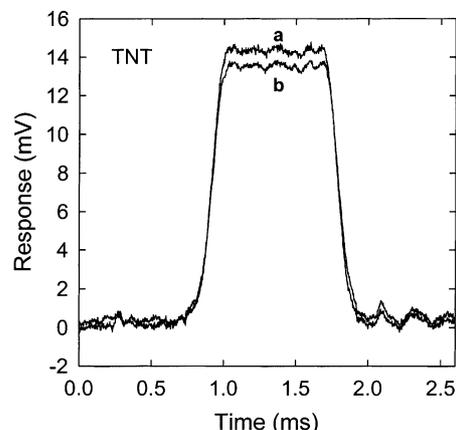


Fig. 11. Photo-induced bending of a gold-coated microcantilever to TNT vapor for the same input photon power for (a) no exposure to TNT molecules; and (b) exposure to TNT molecules.

microcantilever thermal detector allowing to adsorb TNT molecules on the surface of the microcantilever thermal detector. TNT was subsequently removed from the chamber and the microcantilever was exposed to IR radiation. In Fig. 12 we plotted the thermal response of the microcantilever thermal detector (exposed to TNT vapor) from 2.5 to 14.5  $\mu\text{m}$  with TNT molecules adsorbed on the microcantilever surface. As it can be seen in Fig. 12, the photothermal spectrum of the adsorbed TNT exhibits a number of peaks in this wavelength region. These peaks correspond to infrared absorption peaks of TNT vapor.

In order to estimate the number of TNT molecules adsorbed on the microcantilever surface, we measured the resonance frequency of the microcantilever before it was exposed to TNT molecules. However, we observed no measurable change in resonance frequency after TNT molecules adsorbed on the microcantilever surface. We estimated that the resonance frequency shift was than 0.01 Hz, which

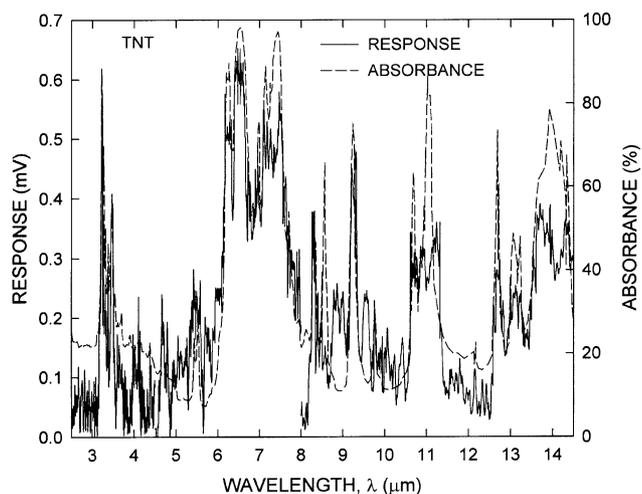


Fig. 12. TNT photothermal spectrum from 2.5 to 14.5  $\mu\text{m}$  obtained using a microcantilever detector with molecules adsorbed on its surface (solid curve). Also plotted is the IR spectrum of TNT (dashed curve).

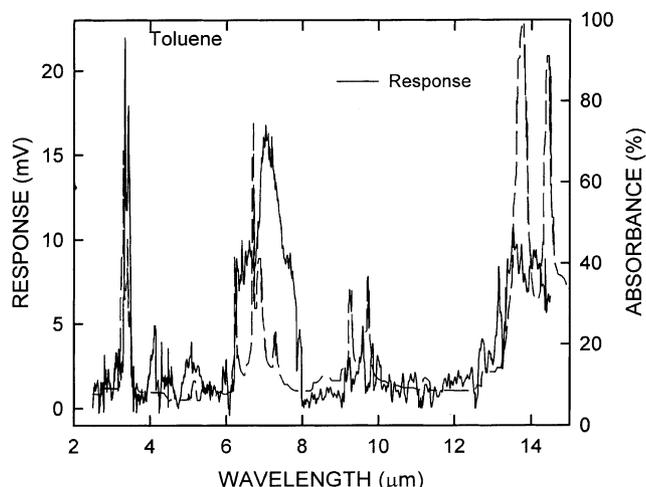


Fig. 13. Toluene photothermal spectrum from 2.5 to 14.5  $\mu\text{m}$  obtained using a gold-coated microcantilever detector with molecules adsorbed on its surface (solid curve). Also plotted is the IR spectrum of toluene (dashed curve).

defines an upper limit of the adsorbed mass of TNT to be less than  $10^{-16}$  g or fewer than  $3 \times 10^7$  of adsorbed molecules.

In Fig. 13 we plotted the photomechanical response of a microcantilever exposed to toluene molecules. The photothermal spectrum of toluene was measured in the wavelength region 2.5 to 14.5  $\mu\text{m}$  (solid curve). We also plotted in Fig. 13, the IR spectrum of toluene (dashed curve).

## 5. Conclusions

The results of the present work demonstrate that photo-mechanical chemical sensors represent an important development in micromechanical chemical detection technology, and can be expected to provide the basis for considerable further development. For example, vastly improved microcantilevers chemical detectors could be produced by making relatively simple changes in the materials and geometries used in microcantilever fabrication. While, the optical readout method used in the present studies is useful with single element designs, practical implementation of microcantilever arrays may require the use of other readout methods, such as piezoresistance or capacitance. Fortunately, the microcantilever technology is compatible with a variety of readout methods and also affords tremendous flexibility to potential system designers.

In this work, we have demonstrated that microcantilevers with various modifying coatings respond sensitively to the presence of chemical analytes. Earlier studies have demonstrated that the mass sensitivities of the frequency variation of microcantilevers can compete with those of other gravimetric chemical sensors. Monitoring the bending of microcantilevers can provide an attractive alternative to detect gas-phase analytes. We have measured the adsorption-induced and photon-induced bending of microcantilevers

exposed to small concentrations of analytes. We believe that the detection limits can be extended to sensitivities below parts per trillion (ppt).

## Acknowledgements

This work was supported by EMSP program of DOE and the Laboratory Director's Research and Development Program of Oak Ridge National Laboratory. Oak Ridge National Laboratory is operated for the US Department of Energy by Oak Ridge National Laboratory, managed by UT-Battelle, LLC, for the US Department of Energy under contract DE-AC05-00OR22725.

## References

- [1] J. Janata, M. Josowicz, D.M. Devaney, *Chemical sensors*, Anal. Chem. 66 (1994) R207.
- [2] J.W. Grate, S.L. Rose-Pehrsson, D.L. Venezky, M.M. Klusty, H.H. Wohltjen, A Smart sensor system for trace of organophosphorous and organosulfur vapor detection employing a temperature-controlled array of surface acoustic waves, Anal. Chem. 65 (1993) 1868.
- [3] J. Brugger, N. Blanc, P. Renaud, N.F. de Rooji, Microlever with combined integrated sensor/actuator functions for scanning force microscopy, Sens. Actuators A 43 (1994) 339.
- [4] E.A. Wachter, T. Thundat, Micromechanical sensors for chemical and physical sensing, Rev. Sci. Instrum. 66 (1995) 3662.
- [5] T. Thundat, G.Y. Chen, R.J. Warmack, D.P. Allison, E.A. Wachter, Vapor detection using resonating microcantilevers, Anal. Chem. 67 (1995) 519.
- [6] G.Y. Chen, T. Thundat, E.A. Wachter, R.J. Warmack, Adsorption-induced surface stress and its effects on resonance frequency of microcantilevers, J. Appl. Phys. 77 (1995) 3618.
- [7] M.K. Baller, H.P. Lang, J. Fritz, C. Gerber, J.K. Gimzewski, U. Drechsler, H. Rothuizen, M. Despont, P. Vettiger, F.M. Battiston, J.P. Ramseyer, P. Fornaro, E. Meyer, H.-J. Güntherodt, A cantilever array-based artificial nose, Ultramicroscopy 82 (2000) 1.
- [8] P.G. Datskos, I. Sauers, Detection of 2-mercaptoethanol using gold-coated micromachined cantilevers, Sens. Actuators B 3016 (2000) 1–8.
- [9] H.P. Lang, M.K. Baller, R. Berger, C. Gerber, J.K. Gimzewski, F.M. Battiston, P. Fornaro, J.P. Ramseyer, E. Meyer, H.-J. Güntherodt, An artificial nose-based on a micromechanical cantilever array, Anal. Chim. Acta 393 (1999) 59.
- [10] D. Sarid, *Scanning Force Microscopy with Applications to Electric, Magnetic, and Atomic Forces*, Oxford University Press, New York, 1991.
- [11] J.H. Hoh, J.P. Cleveland, C.B. Prater, J.-P. Revel, P.K. Hansma, Quantized adhesion detected with atomic force microscope, J. Am. Chem. Soc. 114 (1992) 4917.
- [12] F. Ohnesorge, G. Binnig, True atomic resolution by atomic force microscopy through repulsive attractive force, Science 260 (1993) 1451.
- [13] J. Varesi, J. Lai, T. Perazzo, Z. Shi, A. Majumdar, Photothermal measurements at picowatt resolution using uncooled micro-optomechanical sensors, Appl. Phys. Lett. 71 (1997) 306.
- [14] J.G.E. Harris, D.D. Awschalom, K.D. Maranowski, A.C. Gossard, Fabrication and characterization of 100-nm thick GaAs cantilevers, Rev. Sci. Instrum. 67 (1996) 3591.
- [15] T. Figielski, Photostriction effect in germanium, Phys. Status Solidi 1 (1961) 306.

- [16] R.G. Stearns, G.S. Kino, Effect of electronic strain on photoacoustic generation of silicon, *Appl. Phys. Lett.* 47 (1985) 1048.
- [17] P.G. Datskos, S. Rajic, I. Datskou, Photo-induced and thermal stress in Si microcantilevers, *Appl. Phys. Lett.* 73 (1998) 2319.
- [18] P.G. Datskos, S. Rajic, I. Datskou, C.M. Egert, Novel photon detection-based on electronically-induced stress in silicon, *IR Detectors Focal Plane Arrays V*, SPIE 3978 (1998) 173.
- [19] M. Tabib-Azar, J.S. Leane, Direct control for a silicon microactuator, *Sens. Actuators A21-A23* (1990) 229.
- [20] H.K. Wickramasinghe, R.C. Bray, V. Jipson, C.F. Quate, J.R. Salcedo, Photoacoustics on a microscopic scale, *Appl. Phys. Lett.* 33 (1978) 923.
- [21] P.G. Datskos, S. Rajic, C.M. Egert, I. Datskou, Detection of infrared photons using the electronic stress in metal-semiconductor interfaces, *Infrared Technol. Applications XXV*, SPIE 3698 (1999) 151.
- [22] T. Thundat, E.A. Wachter, S.L. Sharp, R.J. Warmack, Detection of mercury using resonating microcantilevers, *Appl. Phys. Lett.* 66 (1995) 1695.
- [23] T. Thundat, P.I. Oden, P.G. Datskos, G.Y. Chen, R.J. Warmack, in *Microcantilever Sensors*, Oak Ridge, Tennessee, TN, 1996.
- [24] H.P. Lang, R. Berger, C. Andreoli, J. Brugger, M. Despont, P. Vettiger, C. Gerber, J.K. Gimzewski, J.P. Ramseyer, E. Meyer, H.-J. Güntherodt, Sequential position readout from arrays of micromechanical cantilever sensors, *Appl. Phys. Lett.* 72 (1998) 383.
- [25] J.C.L. Britton, R.L. Jones, P.I. Oden, Z. Hu, R.J. Warmack, S.F. Smith, W.L. Bryan, J.M. Rochelle, Multiple-input microcantilever sensors, *Ultramicroscopy* 82 (2000) 17.
- [26] T. Betts, C. Tipple, M. Sepaniak, P.G. Datskos, Selectivity of chemical sensors based on micro-cantilevers coated with polymeric films, *Anal. Chim. Acta* 422 (2000) 89.
- [27] J. Janata, *Principles of Chemical Sensors*, Plenum Press, New York, 1989.
- [28] D.M. Ullevig, J. Evans, Effects of stressed materials on the radial sensitivity function of a quartz crystal microbalance, *Anal. Chem.* 54 (1982) 2341.
- [29] W.D. Bowers, R.L. Chuan, T.M. Duong, A 200 MHz surface acoustic wave resonator mass microbalance, *Rev. Sci. Instrum.* 62 (1991) 1624.
- [30] J.C. Andle, J.F. Valentino, M.W. Lade, D.J. McAllister, in: *An Acoustic Plate Mode Device for Biosensor Applications*, San Francisco, CA, 1991, p. 191.
- [31] J.W. Grate, S.W. Wenzel, R.M. White, Flexural plate wave devices for chemical-analysis, *Anal. Chem.* 63 (1991) 1552.
- [32] F.J. von Preissig, Applicability of the classical curvature-stress relation for thin films on plate substrates, *J. Appl. Phys.* 66 (1989) 4262.
- [33] S. Tomishenko, *Theory of Plates and Shells*, McGraw-Hill, 1940.
- [34] G.G. Stoney, The tension of metallic films deposited by electrolysis, *Proc. R. Soc., Lond. A* 82 (1909) 172.
- [35] P.G. Datskos, S. Rajic, I. Datskou, C.E. Egert, Infrared microcalorimetric spectroscopy using uncooled thermal detectors, *Infrared Imaging*, SPIE 3118 (1997) 280.
- [36] T. Göddenhenrich, H. Lemke, U. Hartmann, C. Heiden, Force microscope with capacitive displacement detection, *J. Vacuum Sci. Technol. A* 8 (1990) 383.
- [37] M. Tortonese, R.C. Barrett, C.F. Quate, Atomic resolution with an atomic force microscope using piezoresistive detection, *Appl. Phys. Lett.* 62 (1993) 834.
- [38] L.J. Kepley, R.M. Crooks, Selective surface acoustic wave-based organophosphonate chemical sensor employing a self-assembled composite monolayer: a paradigm for sensor design, *Anal. Chem.* 64 (1992) 3191.
- [39] A. Dominik, H.J. Roth, W. Gopel, Supramolecular complexes based on calixarenes: force field calculations and applications for chemical sensors, *Supramolecular Sci.* 1 (1994) 11–22.
- [40] K.D. Schiebaum, A. Gerlach, W. Gopel, W.M. Muller, F. Vogtle, A. Dominik, H.J. Roth, Surface and bulk interactions of organic molecules with calixarene layers, *Fresenius J. Anal. Chem.* 349 (1994) 372–379.
- [41] P.I. Oden, P.G. Datskos, T. Thundat, R.J. Warmack, Uncooled thermal imaging using a piezoresistive microcantilevers, *Appl. Phys. Lett.* 69 (1996) 3277.
- [42] P.G. Datskos, P.I. Oden, E.A. Wachter, T. Thundat, R.J. Warmack, Remote infrared detection using piezoresistive microcantilevers, *Appl. Phys. Lett.* 69 (1996) 2986.